Metabolic enzyme expression highlights a key role for MTHFD2 and the mitochondrial folate pathway in cancer

Published in final edited form as:
Nat Commun. 2014 ; 5: 3128. doi:10.1038/ncomms4128.

Metabolic enzyme expression highlights a key role for MTHFD2 and the mitochondrial folate pathway in cancer

Roland Nilsson[1,2,*], **Mohit Jain**[3,4,5,6,*], **Nikhil Madhusudhan**[3,4,5], **Nina Gustafsson Sheppard**[1,2], **Laura Strittmatter**[3,4,5], **Caroline Kampf**[7], **Jenny Huang**[8], **Anna Asplund**[7], and **Vamsi K Mootha**[3,4,5]

[1]Unit of Computational Medicine, Department of Medicine, Karolinska Institutet, 17176 Stockholm, Sweden

[2]Center for Molecular Medicine, Karolinska Institutet, 17176 Stockholm

[3]Broad Institute, Cambridge, Massachusetts 02142, USA

[4]Department of Systems Biology, Harvard Medical School, Boston, Massachusetts 02115, USA

[5]Department of Molecular Biology and the Center for Human Genetic Research, Massachusetts General Hospital, Boston, Massachusetts 02114, USA

[6]Division of Cardiovascular Medicine, Department of Medicine, Brigham and Women's Hospital, Boston, Massachusetts 02115, USA

[7]Department of Immunology, Genetics & Pathology and Science for Life Laboratory, Uppsala University, 75185 Uppsala, Sweden

[8]La Jolla Institute for Allergy and Immunology, San Diego, CA 92037. USA

Abstract

Metabolic remodeling is now widely regarded as a hallmark of cancer, but it is not clear whether individual metabolic strategies are frequently exploited by many tumours. Here we compare messenger RNA profiles of 1,454 metabolic enzymes across 1,981 tumours spanning 19 cancer types to identify enzymes that are consistently differentially expressed. Our meta-analysis

Please address correspondence to: Roland Nilsson, Assistant Professor, Dept. of Medicine, Karolinska Institutet, L8:01 Karolinska University Hospital, 17176 Stockholm, Sweden, +46 722 334 580, roland.nilsson@ki.se. Vamsi K. Mootha, Professor of Systems Biology, Medicine, Harvard Medical School, 185 Cambridge Street, CPZN 7250, Boston, MA 02114, USA, +1 617 643 9710, vamsi@hms.harvard.edu.
*These authors contributed equally to this work

Author contributions

R.N. and M.J. conceived of and performed all experiments, collected and analyzed experimental data, and prepared the manuscript. N.M., L.S. and J.H. performed shRNA mediated knockdown experiments, cell proliferation and biochemical assays. N.G.S. performed siRNA mediated knockdown experiments, cell proliferation and cell death assays. C.K. and A.A performed immunohistochemistry experiments. V.K.M conceived of all experiments, reviewed all experimental data and prepared the manuscript. All authors have discussed the results and reviewed the manuscript.

Competing financial interests

The Massachusetts General Hospital has filed a provisional patent application listing R.N., M.J., and V.K.M. entitled "**Glycine, mitochondrial one-carbon metabolism, and cancer", patent number 61/791,082**. All remaining authors declare no competing financial interests.

recovers established targets of some of the most widely used chemotherapeutics, including dihydrofolate reductase, thymidylate synthase and ribonucleotide reductase, while also spotlighting new enzymes, such as the mitochondrial proline biosynthetic enzyme *PYCR1*. The highest scoring pathway is mitochondrial one-carbon metabolism and is centred on *MTHFD2*. *MTHFD2* RNA and protein are markedly elevated in many cancers and correlated with poor survival in breast cancer. *MTHFD2* is expressed in the developing embryo, but is absent in most healthy adult tissues, even those that are proliferating. Our study highlights the importance of mitochondrial compartmentalization of one-carbon metabolism in cancer and raises important therapeutic hypotheses.

Introduction

Divergent metabolism in tumors was first recognized nearly a century ago [1], and is consistently observed across a number of tumor types, and has been exploited for diagnostic as well as therapeutic purposes. For example, rapid glucose consumption in tumors may be imaged by positron emission tomography (PET) and used to diagnose malignancy and to monitor the response to therapy [2]. Furthermore, the dependence of cancer cells on nucleotide metabolism forms the basis for the use of several common chemotherapeutics, including agents targeting dihydrofolate reductase (DHFR), thymidylate synthase (TYMS) and ribonucleotide reductase (RRM2) [3]. Moreover, recent data has suggested that many of the growth factor signaling pathways commonly perturbed in cancer impinge on metabolic enzymes [4], as well as that metabolic enzymes may act as *bona fide* oncogenes [5] and even transform cells [6]. Collectively, these observations underscore the need for a deeper understanding of metabolic reprogramming in cancer. While classic biochemical studies have identified a number of enzymes whose activities are increased in cancers [7,8], the complex, coordinated changes in metabolism that occur during cancer transformation have only begun to be understood [9].

Over the past decade, a wealth of data on tumors, normal tissues and cell models have been generated using microarrays and analyzed to identify genes differentially expressed in cancer [10,11]. These data provide a unique opportunity to study expression patterns of metabolic enzymes in cancer and thereby define the metabolic program of cancer on a genome-wide scale [9]. Yet, as most studies have compared tumor tissue to a quiescent, postmitotic normal control tissue, these analyses do not indicate whether enzymes over-expressed in tumors are also active in proliferative normal tissues. Identification of cancer-specific metabolic activities is essential, as current chemotherapeutic agents target metabolic enzymes found both in transformed cells as well as normal proliferating cells, notably immune cells, hair follicles and intestinal epithelium, resulting in the on-target side effects in proliferative tissues that limit these agents' therapeutic index [3].

Here we report a systematic re-analysis of previously published microarray datasets, focusing on genes known or predicted to encode metabolic enzymes, and identify several enzymes and pathways consistently over-expressed or under-expressed across a large number of different cancer types. In particular, we find that enzymes of the mitochondrial folate metabolic pathway, which are ordinarily low or absent in normal adult tissues, are

highly upregulated in cancer. Finally, we show that the MTHFD2 enzyme in this pathway is highly expressed on the protein level in a variety of human tumors and negatively correlates with survival in breast cancer patients.

Results

Meta-analysis of enzyme mRNA expression in human tumors

To systematically investigate expression of metabolic pathways across multiple tumor types, we first searched the GeneChip Oncology Database (GCOD) [10] for studies containing primary tumor tissue samples and suitable normal tissue controls. We found 51 independent datasets satisfying this criterion, covering a total of 1,981 tumors of 19 different types *vs.* 931 matched normal tissue controls (Supplementary Data 1), and interrogating a total of 20,103 genes. To avoid artifacts from comparison across different array platforms and laboratories, we calculated differential expression (quantified by Z-scores) within each dataset, and estimated statistical significance for each gene by permutation tests. While the extent of differential expression varied widely across studies (Fig. 1a) — likely reflecting variability in tumor types, nature of the control tissue, and experimental design — we reasoned that genes consistently differentially expressed across these cancers would represent processes of fundamental importance to transformed cells. We therefore scored each gene by counting the number of datasets where differential expression was detected at a 5% false discovery rate (Fig. 1b, full genome wide analysis available as Supplementary Data 2). Most high-scoring over-expressed genes have previously been found to be expressed in the “committed” S, G2 and M phases of the cell cycle [12,13], where cells are thought to be most vulnerable to pharmacologic intervention. This likely reflects the high proportion of proliferating cells in tumors compared to control tissues.

We focused our analysis on 1,454 metabolic enzymes annotated in a previously established model of the human metabolic network [14]. Among the top 50 consistently over-expressed enzymes (Table 1), we recovered several metabolic pathways previously associated with cancer, including multiple enzymes involved in glycolysis [15], *de novo* synthesis and salvage of nucleotides [7] and in particular deoxynucleotides, as well as prolyl hydroxylases responsive to hypoxia [16] and glycosylation enzymes [17] (Fig. 1c, d), in agreement with a recent independent study [9]. Among these metabolic enzymes, we recovered a number of genes targeted by existing cancer therapeutics, including *DHFR* (the target of methotrexate), *TYMS* (the target of 5-fluorouracil), and *RRM2* (the target of gemcitabine) (Fig. 1b, Table 1). Beyond metabolic enzymes, our analysis also identified a number of other enzyme targeted by chemotherapeutics, including topoisomerase 2A (*TOP2A*), aurora A kinase (*AURKA*), and cyclin-dependent kinase 4 (*CDK4*) (Fig 1b, Supplementary Data 2), as consistently over-expressed in cancers. Hence, our systematic analysis of metabolic reprogramming identifies a number of establish cancer-related metabolic enzymes and pathways across varied tumor types.

Our analysis additionally reveals several metabolic enzymes consistently under-expressed in cancer and whose roles in cancer have not been previously appreciated. Among the metabolic enzymes consistently underexpressed in cancer (Table 2), we noted a number of enzymes related to fatty acid metabolism, including catabolism of branched fatty acids

(*ACOX2*, *ETFDH*), synthesis of ketones (*HMGCS2*) and fatty acid synthesis (*ACCB*). A number of antioxidant enzymes were also consistently down-regulated in cancer (Fig. 1c, Table 2). Taken together, these findings suggest consistent down-regulated metabolic pathways and enzymes across multiple tumor types which remain to be explored.

Cancer cells have previously been proposed to exhibit stem cell like properties, expressing genes characteristically found in embryonic cells [18]. Of the 35 enzymes previously established to be expressed by embryonic stem cells [18], a large fraction were over-expressed in tumors (Fig. 1e), suggesting a tendency to revert to a embryonic-like metabolic program. Among the top 50 consistently over-expressed enzymes (Table 1) identified in our study, 26 enzymes have previously been evaluated using large-scale RNAi screening to determine those essential for tumorgenesis *in vitro* and *in vivo* in breast cancer cells [19]. Among these 26 metabolic genes, 6 genes (*CTPS*, *GAPDH*, *PYCR1*, *MTHFD2*, *TPI1*, and *TSTA3*) were found to be require for tumorgenesis *in vitro* and 5 genes (*CTPS*, *GAPDH*, *GMPS*, *PYCR1* and *TPI1*) *in vivo* [19]. Whereas several of these genes are components of glycolytic or nucleotide metabolism pathways previously associated with tumorgenesis, *TSTA3*, *PYCR1*, and *MTHFD2* are members of pathways less appreciated in the context of cancer. *TSTA3* catalyzes the production of GDP-L-fucose (Fig. 1c), which serves as the substrate for fucosyltransferases reactions. Increased levels of GDP-L-fucose and fucosylated glycoproteins have been noted in cancer [20], their role in tumorgenesis remains unclear. Similarly, our analysis also identified the mitochondrial enzyme *PYCR1* (Fig. 1c), an established target of the oncogene myc [21]. *PYCR1* catalyzes the final step of proline synthesis from glutamate (Fig. 1c), including in cancer cells [22]. In conjunction with its cytosolic isoform, *PYCR1* may serve as a cycle for the transfer of reducing equivalents from the cytosol into the mitochondria [23], modulating both intracellular redox status [24] and sensitivity to oxidant injury [25].

Among all 1,454 enzymes examined, the metabolic enzyme most consistently overexpressed in tumors was the mitochondrial folate-coupled dehydrogenase *MTHFD2* (Fig. 1a, b), ranked within the top 3 of all 20,103 genes interrogated (Supplementary Data 2). *MTHFD2* is integral to mitochondrial one-carbon metabolism (Fig. 1d), a metabolic system recently implicated in rapid cancer cell proliferation [26]. *MTHFD2* is a bifunctional enzyme, catalyzing the NAD^+ dependent CH_2-THF dehydrogenase and CH^+-THF cyclohydrolase reactions within the mitochondria [27]. Within mitochondrial one-carbon metabolism, we also noted frequent overexpression of the preceding enzyme, *SHMT2*, which catalyzes the production of glycine and one-carbon groups in the form of CH_2-THF from serine (Fig. 1d). The subsequent enzyme, *MTHFD1L*, catalyzing the synthesis of formate and regeneration of the THF cofactor (Fig. 1d), was only measured on 11/51 microarrays, so that our meta-analysis was not well-powered in this case; however, it appeared consistently over-expressed in those 11 datasets (data not shown). In the paralogous cytosolic one-carbon pathway, the $NADP^+$-linked, trifunctional *MTHFD1* enzyme also exhibited over-expression in multiple cancers, although it did not reach top 50 threshold (Fig. 1d). This is consistent with the notion that the mitochondrial one-carbon system serves to produce formate which is then again coupled to THF in the cytosol by the *MTHFD1* enzyme [27]. Interestingly, the cytosolic enzyme *ALDH1L1*, which breaks down cytosolic formyl-THF into CO_2 and THF

and thus opposes the synthesis of one-carbon units, was consistently under-expressed in tumors (Fig. 1d, Table 1). The paralogous mitochondrial enzyme, *ALDH1L2* was not reliably measured on the microarray platforms used (Fig. 1d). The aminomethyltransferase *AMT*, a component of the enzyme system that catabolizes glycine, was also under-expressed (Fig. 1d, Table 2). These findings suggest that the metabolic pathway channeling one-carbon units through the mitochondria via *MTHFD2* has an important role in cancer biology.

Enzymes in transformed and normal proliferating cells

Many of the metabolic changes accompanying transformation are also active in normal proliferating cells [4]. To identify cancer-related metabolic enzymes more specific to the transformed state, we analyzed gene expression from 80 normal human tissues, including proliferative tissues such as intestine and bone marrow, compared to transformed cell lines. The well-known chemotherapeutic targets *DHFR, RRM2, TYMS* and *TOP2A* were expressed in several normal proliferating cell types (Fig. 2a), in which the adverse side-effects of drugs targeting these enzymes are commonly observed. In contrast, *MTHFD2* exhibited little expression in these tissues, and was in fact the most cancer-specific mRNA measured on these arrays, as quantified by a transformed/normal expression ratio (Fig. 2b). In this analysis we also noted the *PYCR1* enzyme (Fig. 2b), which was also among the most commonly over-expressed enzymes in cancer (Table 1). *MTHFD2* was not detected upon activation of serum-stimulated normal human fibroblasts *in vitro*, nor in hepatocytes proliferating *in vivo* in response to partial liver resection (Fig. 2c), whereas other established chemotherapeutic drug targets were induced also in these normal proliferating cells. However, we did observe *MTHFD2* induction at an early time point in activated lymphocytes (Fig. 2c), consistent with previously observed *MTHFD2* activity in bone marrow [28], indicating a possible role for *MTHFD2* in normal hematopoietic cells.

The *MTHFD2* enzymatic activity has also previously been detected in embryonic fibroblasts from the mouse [28] as well as in human embryonic stem cells [18], and knockout of the gene is embryonic lethal in mice [29]. We found that the *MTHFD2* mRNA increases during the initial rounds of cellular division in both mouse and human fertilized oocytes (Fig. 2d). In addition, expression is high in mouse fetal liver and hypothalamus, but decreases markedly around birth (Fig. 2e). These observations support a role for the enzyme in embryonic development.

RNA interference targeting MTHFD2 causes cancer cell death

To further evaluate whether expression of the *MTHFD2* gene product is required for cancer cell proliferation, we used two different RNAi modalities to silence *MTHFD2* across 16 diverse cancer cell types. In total, we used 2 lentiviral delivered shRNA hairpins and 6 sequence-independent non-viral delivered siRNA oligonucleotides (Supplementary Fig. 1–2). *MTHFD2* mRNA, protein levels, and enzymatic activity were substantially reduced by shRNA (Supplementary Fig. 1a–c, 3) or siRNA targeting *MTHFD2* (Supplementary Fig. 1e). In most cell lines, proliferation was severely reduced, consistent with prior observations [19], with noted variability in the degree of defect among the various cell lines (Supplementary Fig. 1d, 1f). Propidium iodide staining and flow cytometry revealed marked cell death at the 48 hour time point, with 40% of cells nonviable (Supplementary Fig. 1g, h), while non-targeting control siRNA transfections did not impair cell viability (Supplementary

Fig. 1i). While RNAi-mediated loss of the *MTHFD2* gene product was associated with slowed cancer cell proliferation and marked cell death, we have hitherto been unable to rescue this phenotype by exogenous expression of the *MTHFD2* cDNA, which is required to definitively prove the effect is due to the enzymatic activity of MTHFD2 protein and not a consequence of silencing its RNA or an off-target effect.

MTHFD2 protein expression in tumors and normal tissues

To evaluate if the MTHFD2 protein is overexpressed in human tumors, we performed immunohistochemistry in 176 tumor samples, collected from 16 tumor types. Strong or moderate staining for MTHFD2 was observed in 12 of these of tumor types, and the protein was detectable in all cancer types with the exception of gliomas (Fig. 3a). While staining intensity was variable across tumor samples, the protein consistently appeared specific to transformed cells within the tumors, with little or no staining seen in adjacent stroma (Fig. 3b). These data indicate that the MTHFD2 protein is indeed present in multiple cancer types. Activity of the enzyme has also previously been observed in transformed cell lines [30]. We did observe staining in normal epithelium of the gut tissues, in particular in intestinal crypts containing stem cells, in tonsil lymphoid tissue and in exocrine pancreas (Supplementary Fig. 4). Finally, we evaluated the expression of *MTHFD2* in six independent cohorts of patients with breast cancer followed for survival. Whereas there was heterogeneity among individual data sets (Supplementary Fig. 5a), likely reflecting differences in the number of patients and clinical parameters including, entry patient criteria and treatment strategies, a meta-analysis of all six independent cohorts indicated that high expression of the *MTHFD2* mRNA was associated with increased mortality in breast cancer patients (Supplementary Fig. 5b), suggesting a potential role in tumor progression.

Discussion

In this study we have identified metabolic enzymes and pathways that are frequently over-expressed in tumors, and demonstrated that one of these enzymes, *MTHFD2*, is broadly required for cancer cell proliferation and viability. It should be emphasized that our meta-analysis only addresses changes in enzyme expression at the mRNA level, and our results do not exclude that other enzymes may be dysregulated in cancer by post-transcriptional mechanisms such as translational control or allosteric regulation. Moreover, while our meta-analysis was designed to reliably detect genes that are frequently over-expressed in tumors, it will likely miss genes absent or not well measured on common microarray platforms, and does not consider tissue-specific phenomena. Future studies investigating differences in metabolic enzyme expression between tumor types, as well as co-occurrence of enzymes and pathways in tumors, would be a valuable extension to this work.

Within our systematic analysis of metabolic reprogramming, we identified a number of metabolic genes whose expression was altered in a variety of tumor types relative to normal controls. Among the metabolic enzymes that were consistently over-expressed in tumors (Table 1), we find a high proportion of established cancer-related metabolic enzymes and known chemotherapeutic drug targets, suggesting that the additional enzymes identified here may be of interest as cancer targets as well. These additional enzymes include *MTHFD2* and

PYCR1, both of which are low or absent in a large panel of normal tissues, including the proliferative tissues of the gut and a number of immune cell types; this could theoretically limit on-target side effects typically associated with these cell types. We further demonstrate the necessity of the *MTHFD2* gene in cancer cell proliferation and survival across a number of cancer cell lines. While the proliferation defect and early cell death phenotypes with *MTHFD2* knockdown were observed with multiple independent RNAi sequences, we cannot definitively rule out off target RNAi effects. Moreover, while our results indicate a requirement for the *MTHFD2* mRNA, further studies are needed to prove that the MTHFD2 protein and its enzymatic activity are indeed mediating the observed effects on cancer cell proliferation.

Genes consistently under-expressed in tumors include metabolic enzymes involved in fatty acid metabolism, including catabolism of branched fatty acids, and ketogenesis as well as a number of antioxidant enzymes (Table 2). The consistent repression of these metabolic enzymes suggest a larger metabolic reprogramming that occurs with transformation in varied tumor types, and may reflect an effort on the part of a cancer cell to shunt metabolites to particular biosynthetic pathways rather than catabolism, to limit production of toxic intermediates, and / or to preferentially shuttle reducing equivalents to particular compartments, such as the mitochondria. As with the over-expressed metabolic genes, further investigation of these under-expressed metabolic enzymes may uncover metabolic vulnerabilities which may be targeted therapeutically.

While the enzymatic function of the MTHFD2 enzyme is well established, its broader role in cancer cell metabolism is not yet clear. Interestingly, while *SHMT2* knockdown renders cancer cells auxotrophic for glycine [26], we find that *MTHFD2* knockdown results in death of human cancer cells in complete medium containing glycine (Supplementary Fig. 1g,h). This observation indicates that the observed cell death upon loss of *MTHFD2* is not due to blocking of glycine synthesis. Moreover, as *SHMT2* is thought to be the main source of mitochondrial one-carbon units, this observation also suggests that depletion of formate, the other main metabolic product of the mitochondrial one-carbon pathway, is unlikely to be the cause of cell death upon loss of MTHFD2. In support of this hypothesis, we have been unable to rescue the *MTHFD2* defect with exogenous formate. Moreover, both normal and transformed mouse embryonic fibroblasts lacking *MTHFD2* are viable but auxotrophic for glycine [31], suggesting that the strict dependence on *MTHFD2* may be unique to human cells. A recent report indicates that RNAi targeting *MTHFD2* also affects cell migration and invasion of human cancer cells. [32]

The cell death observed upon MTHFD2 depletion may therefore be due to some type of toxic event that does not arise in wild type cells and is unrelated to normal cellular metabolism. One hypothesis is that, since MTHFD2 is considered required for recycling the THF cofactor in mitochondria (Fig 1c), loss of the protein could result in mitochondrial folates becoming “trapped” in the CH_2-THF form, which would be detrimental to all folate-coupled activities in the mitochondria. In addition, because CH_2-THF cannot be transported out of the mitochondria [27], folate trapping within the mitochondria with MTHFD2 silencing could potentially impact a number of folate-dependent cytosolic reactions, as well. A similar “folate trap” phenomenon has been observed upon loss of cytosolic folate-coupled enzymes,

including loss of methionine synthase [33]. Alternatively, loss of MTHFD2 could result in accumulation of an hitherto unknown toxic metabolite that rapidly causes cell death, perhaps from unwanted side-reactions of metabolic enzymes occurring in the absence of MTHFD2 [34]. While we have consistently observed cell death in response to several independent RNAi sequences targeting *MTHFD2*, it must be emphasized that we have hitherto not been able to rescue cell death by overexpression of an RNAi-resistant *MTHFD2* cDNA, which is required to conclusively demonstrate that loss of this protein causes cancer cell death.

While additional experiments are needed to understand the role of *MTHFD2* function in embryonic cells and in cancer, the specific expression of *MTHFD2* in transformed cells relative to other adult tissues, and the growth and survival defects caused by loss of the mRNA suggests that this enzyme should be evaluated as a potential target for cancer chemotherapeutics. More generally, the current analysis, combined with our previous report [26] and other recent studies [6,19] points to a remodeling of mitochondrial one carbon metabolism in cancer. Although it has long been appreciated that one-carbon folate metabolism is compartmentalized within human cells, these recent studies indicate that compartment-specific alterations may be critical to promoting cancer growth and survival. The recognition that compartmentalization of one-carbon folate metabolism is altered in cancer raises new opportunities for identifying novel therapies for cancer, as well as for targeting with greater precision existing anti-folate therapies.

Methods

Microarray data analysis

Microarray data sets were selected from the GeneChip Oncology Database [10] (GCOD) according to the following criteria: we considered only data sets of human tumors with normal tissues samples as controls, excluding cell lines and cultured normal cells; we required at least 3 independent samples in both tumor and control groups; and we considered only data from the Affymetrix HG-Focus, HG-U133A, HG-U133Av2, HG-U133+v2, HG_U95A, and HG_U95Av2 microarray platforms. A list of data sets included is provided in Supplementary Data 1. All data sets were uniformly processed from the Affymetrix CEL using the Robust multi-array average (RMA) algorithm, as described [10]. For each microarray platform, in cases of multiple probesets per gene, we selected the probeset with maximal mean signal rank across all arrays. Differential expression between tumor and normal groups was quantified for each data set using Z-scores, and nominal P-values of differential expression were calculated for each gene using a permutation test (1,000 permutations). False discovery rates (FDR) were computed using the Benjamini-Hochberg procedure [35]. Meta-analysis of FDR was done by counting the number of times a gene was over-expressed in tumors and subtracting the number of times it was under-expressed. Enrichment analysis was done using the GSEA-p method [36] with the parameter p set to 1.

The compendium of 80 human tissues was generated from duplicate samples for each tissue using Affymetrix U133A arrays [37]. The gcRMA-normalized data was downloaded from www.biogps.org, and duplicates were averaged for the analysis presented in Figure 2. Our

classification of tissues and cells as normal/postmitotic, normal/proliferating or transformed is described in Supplementary Table 1.

Expression data from proliferating human fibroblasts, human T cells, mouse regenerating liver and mouse/human embryonic development was obtained from the NCBI Gene Expression Omnibus, series accession GSE3945, GSE2770, GSE6998, and GSE18290, respectively. No additional normalization was performed.

Cell culture

Human cancer cell lines (passage number 5–18 in all cases except HCT-116) were obtained from the National Cancer Institute (NCI). All cell lines were cultured in RPMI-1640 medium (Invitrogen) with 2 mM L-glutamine and 5% fetal bovine serum (HyClone Laboratories). Cells were cultured at 37°C in 5% CO_2.

shRNA knockdown of MTHFD2

Cells were cultured according to standard techniques as described above. Lentiviral vectors (pLKO.1) expressing shRNA clones were generated by the Broad RNAi Consortium, as previously described [26]. Sequence-independent shRNA's were generated against human *MTHFD2* (sh50, sh53) or a control sequence (shCtrl) not matching any human gene. Accession numbers are: shCtrl, Clone ID TRCN0000072232, Clone name lacZ_27s1c1, Target sequence CGTCGTATTACAACGTCGTGA; shD2-50, Clone ID TRCN0000036550, Clone name NM_006636.2-548s1c1, Target sequence CGAATGTGTTTGGATCAGTAT; shD2-53, Clone ID TRCN0000036553, Clone name NM_006636.2-772s1c1, Target sequence GCAGTTGAAGAAACATACAAT. The pLKO.1 plasmids were each packaged with VSVG and pCMV-dR8.91 vectors in 293T cells to generate lentivirus, as previously described [26]. One day prior to transfection, 850,000 293T cells were seeded per well/plasmid. Roche X-tremeGENE 9 was used to transfect 293T cells according to the manufacturer's protocols (100 ng VSVG, 900 ng pCMV-dR8.91, and 1 ug plasmid with 6 uL transfection reagent for each well/plasmid). 18 hours after transfection, high serum (30% Gibco 16000 FBS in DMEM) media was added. Virus was harvested at 24 and 48 hours, pooled, and frozen at −80C in single-use aliquots[26].

Lentiviral infection was performed as previously described [26]. Cells were seeded at a density of 1500–2500 cells per well, depending on cell type, in a 96-well plate in RPMI 1640 medium (200 μL total) supplemented with 5% fetal bovine serum and 2mM glutamine. Fifteen hours after plating, cell culture medium was exchanged with fresh medium containing Polybrene (8 μg/mL) and viral supernatant. Plates were centrifuged for 30 minutes at 2000 rpm and 37°C, after which the medium was replaced. Twenty-four hours later, cells were selected for infection by adding puromycin to cell culture medium (2 μg/ml). Uninfected control cells demonstrated 100% cell death within 48 hours. Seven days following plating, cells were washed with PBS and fixed using 4% paraformaldehyde for 20 minutes at room temperature. Cells were stained using Hoechst 33342 dye (Invitrogen) according to manufacturer's specifications, imaged using ImageXpress Micro (Molecular Devices), and counted using the "count nuclei" module of MetaXpress (Molecular Devices).

Cell counts are expressed normalized to shCtrl infected cells for each cell line. All experiments were performed using at least four independent cell cultures.

For *MTHFD2* mRNA and protein measurements following shRNA knockdown, HCT116 cells were infected with lentiviral shRNA vectors in 6-well dishes as described [26]. Seven days following infection, mRNA was isolated from cells using an RNeasy kit (Qiagen), and qRT-PCR was performed for *MTHFD2* and HPRT using the Taqman assays (Applied Biosystems, assay ID Hs01074341_g1 and Hs99999909_m1, respectively), according to manufacturer's instructions. qRT-PCR data is expressed as $\Delta\Delta C_T$ values. For western blot analysis, whole cell lysates were prepared and resolved by SDS-PAGE, followed by transfer to a PVDF membrane using the Trans-Blot Turbo Transfer System. Membranes were stained using primary antibody for ATP5A (Abcam Mouse Monoclonal, no. AB147480, 1:100,000) or MTHFD2 (Abcam Mouse Monoclonal, no. AB56772, 1:500), followed by secondary antibody (Polyclonal Sheep anti-IgG mouse antibody, no. NA931V, 1:10,000). Signal was detected using enhanced chemiluminescence. Full images of western blots are provided in Supplementary Fig. 3a. For assay of MTHFD2 activity, 1×10^6 cells were lysed using 1% Triton-X and MTHFD2 activity was measured in lysate as previously described[28].

Transient siRNA knockdown

siRNA oligonucleotides targeting *MTHFD2* were from Dharmacon, catalog# J-009349-10, J-009349-11, J-009349-12, D-009349-02, D-0093848-03 and D-009349-04; referred to in this study as siD2-10, siD2-11, siD2-12, siD2-2, siD2-3 and siD2-3, respectively. Control siRNAs were Dharmacon ON-TARGET, referred to as siCtrl1, and Dharmacon siGenome, referred to as siCtrl-2. Cells were transfected 24 hrs after seeding (at 40–60% confluence) with 10 nM oligonucleotide, using the INTERFERin transfection reagent (Polyplus Transfection). Western blot analysis was performed on cells seeded at 150,000 cells/well in a 6-well plate and lysed in 2x Laemmli sample loading buffer 48 hours h after siRNA transfection. Lysates were separated by 10% Mini-PROTEAN® TGX™ Precast Gel (Bio-Rad), transferred to 0.45 μm nitrocellulose membrane (Bio-Rad) and blocked in 5% milk in TBST. The following antibodies were used for immunoblotting: monoclonal mouse β-actin antibody (Sigma-Aldrich, 1:30,000), monoclonal mouse MTHFD2 (Abnova, no. H00010797-M01, 1:500) and anti-Mouse IgG (H+L) HRP conjugated (Pierce, 1:100,000). Full images of western blots are provided in Supplementary Fig. 3b.

For assessment of cellular proliferation following transient siRNA transfection, cells were seeded at 4,000 cells/well in a 96-well plate 24h prior to siRNA transfections and lysed at indicated time points using CyQuant Cell Proliferation Assay (Invitrogen) according to manufacturer's instructions. Binding of CyQuant to DNA was analyzed by measuring fluorescence in a VICTOR2 plate reader (PerkinElmer).

Flow cytometric measurement of cell death

Cells were seeded at 10^6 cells/100mm dish 24h prior to siRNA transfections. Cells were collected by trypsinization at indicated time-points, pelleted for 5 min at 1500 rpm, rinsed twice in ice-cold PBS and then resuspended in 0.01 M HEPES/NaOH (pH 7.4), 0.14 M NaCl, 2.5 mM $CaCl_2$. Cell suspension was diluted to a concentration of 5×10^5 cells/mL;

2.5×10^5 cells were transferred to a 5 mL culture tube and Propidium Iodide (PI, BD PharMingen) was added to a concentration of 0.5 ug/mL; cells were gently vortexed and incubated for 15 min at 25°C in the dark. Samples were analyzed within 1 hrs in a CyAn ADP Analyzer (Beckamn Coulter), with flow rate approximately 300 events / s and a total of 25,000 events were gated. Debris and doublets were excluded using forward scatter and pulse width before gating of PI-positive populations.

Immunohistochemistry

Specimens containing normal and/or cancer tissues were collected in accordance with approval from the local ethics committee (ref # Ups 02-577) and according to Swedish rules and legislation. Tissue microarrays holding samples from the different cancer types as well as from normal tissues were produced as previously described [38]. Briefly, tissue samples were fixed with formalin and embedded in paraffin; 2–3 tissue cylinders from representative areas were punched out and assembled in a recipient tissue microarray block with pre-punched holes. 4 μm sections were then cut and placed on Superfrost Plus microscope slides (Thermo Fisher Scientific, Fremont, CA, USA) for immunohistochemical staining. Slides were deparaffinized in xylene, hydrated in graded alcohols and blocked for endogenous peroxidase for 5 min in 0.3% H_2O_2 diluted in 95% ethanol. Heat-induced epitope retrieval was done in a decloaking chamber (Biocare Medical) with citrate buffer at pH 6.0 for 4 min at 125° C. Before staining, slides were immersed in wash buffer containing 0.2% Tween-20 for 15 min to avoid surface tension. Staining was performed in an Autostainer 480S instrument (Thermo Fisher Scientific) at room temperature with the following steps: Ultra V block (Thermo Fisher Scientific, no. TA-125-UB) 5 min, primary antibody 30 min, primary antibody enhancer (Thermo Fisher Scientific, no. TL-125-PB) 20 min, UltraVision LP HRP polymer (Thermo Fisher Scientific, no. TL-125-PH) 30 min, and diaminobenzidine (Thermo Fisher Scientific, no. TA-125-HDX) 5 min × 2 times. MTHFD2 primary antibody was from Abnova (mouse monoclonal, no. H00010797-M01). Between incubations, slides were rinsed in wash buffer. Slides were counter-stained with Mayer's hematoxylin (Histolab, Gothenburg, Sweden, ref. 01820), dehydrated and mounted on cover slips using pertex (Histolab, ref. 00871.0500). Two independent observers evaluated staining for all samples, blinded to the identity of the antibodies used. Staining intensity was classified (negative, weak, moderate, strong) and fraction of positive cells (0, <25%, 25–75%, >75%) were estimated separately for tumor cells and tumor stroma.

Survival analysis

Six independent large cohorts of cancer patients for which survival data for at least a decade was available were examined. Microarray data from Chin et al. [39] and van de Vijver et al. [40], were downloaded from the Lawrence Berkeley National Laboratory (http://cancer.lbl.gov/breastcancer/list_data.php?id=9) and Rosetta Inpharmatics (http://www.rii.com/publications/2002/nejm.html), respectively. Microarray data from the Desmedt et al. [41], Pawitan et al. [42], Miller et al. [43] and Kao et al. [44] studies are available from the NCBI Gene Expression Omnibus, accessions GSE7390, GSE1456, GSE3494, and GSE20685, respectively. Survival data and clinical parameters were obtained from the original reports. Patients were split into "positive" or "negative" based on above- or below-median expression of the *MTHFD2* mRNA, and Kaplan-Meier curves were derived for these groups. Hazard ratios were

estimated using Cox's proportional hazard model [45]. Groups were tested for significant differences using the logrank test and meta-analysis was performed using the method of DerSimonian and Laird [46].

Supplementary Material

Refer to Web version on PubMed Central for supplementary material.

Acknowledgments

We acknowledge the National Cancer Institute for cellular reagents. We acknowledge Joseph White (Dana-Farber Cancer Institute) for assistance with the GCOD database. R.N. and N.G.S. were supported by grants from the Swedish Research Council (K2012-99X-22007-01-3) and Foundation for Strategic Research (ICA10-0023). M.J. was supported by NIH K08HL107451. This work was funded by grants from the NIH (R01DK081457). V.K.M. is an Investigator of the Howard Hughes Medical Institute.

References

1. Warburg O. Über den Stoffwechsel der Carcinomzelle. Naturwissenschaften. 1924; 12:1131–1137.
2. Ben-Haim S, Ell P. 18F-FDG PET and PET/CT in the evaluation of cancer treatment response. Journal of nuclear medicine3: official publication, Society of Nuclear Medicine. 2009; 50:88–99.
3. Tennant, Da; Durán, RV.; Gottlieb, E. Targeting metabolic transformation for cancer therapy. Nature reviews cancer. 2010; 10:267–77.
4. DeBerardinis RJ, Lum JJ, Hatzivassiliou G, Thompson CB. The biology of cancer: metabolic reprogramming fuels cell growth and proliferation. Cell metabolism. 2008; 7:11–20. [PubMed: 18177721]
5. Yan H, et al. IDH1 and IDH2 mutations in gliomas. New England Journal of Medicine. 2009; 360:765–773. [PubMed: 19228619]
6. Zhang WC, et al. Glycine Decarboxylase Activity Drives Non-Small Cell Lung Cancer Tumor-Initiating Cells and Tumorigenesis. Cell. 2012; 148:259–272. [PubMed: 22225612]
7. Weber G. Biochemical strategy of cancer cells and the design of chemotherapy: GHA Clowes Memorial Lecture. Cancer research. 1983; 43:3466–3492. [PubMed: 6305486]
8. Weinhouse S. Glycolysis, respiration, and anomalous gene expression in experimental hepatomas: G.H.A. Clowes memorial lecture. Cancer research. 1972; 32:2007–16. [PubMed: 4343003]
9. Hu J, et al. Heterogeneity of tumor-induced gene expression changes in the human metabolic network. Nature Biotechnology. 2013; 1–1010.1038/nbt.2530
10. Liu F, White Ja, Antonescu C, Quackenbush J. GCOD - GeneChip Oncology Database. BMC bioinformatics. 2011; 12:46. [PubMed: 21291543]
11. Rhodes DR, et al. Large-scale meta-analysis of cancer microarray data identifies common transcriptional profiles of neoplastic transformation and progression. Proceedings of the National Academy of Sciences of the United States of America. 2004; 101:9309–14. [PubMed: 15184677]
12. Whitfield ML, et al. Identification of genes periodically expressed in the human cell cycle and their expression in tumors. Molecular Biology of the Cell. 2002; 13:1977–2000. [PubMed: 12058064]
13. Cho RJ, et al. Transcriptional regulation and function during the human cell cycle. Nature genetics. 2001; 27:48–54. [PubMed: 11137997]
14. Duarte NC, et al. Global reconstruction of the human metabolic network based on genomic and bibliomic data. Proceedings of the National Academy of Sciences of the United States of America. 2007; 104:1777–82. [PubMed: 17267599]
15. Altenberg B, Greulich KO. Genes of glycolysis are ubiquitously overexpressed in 24 cancer classes. Genomics. 2004; 84:1014–20. [PubMed: 15533718]
16. Hofbauer KH, et al. Oxygen tension regulates the expression of a group of procollagen hydroxylases. European Journal of Biochemistry. 2003; 270:4515–4522. [PubMed: 14622280]

17. Dennis JW, Granovsky M, Warren CE. Glycoprotein glycosylation and cancer progression. Biochimica et biophysica acta. 1999; 1473:21–34. [PubMed: 10580127]
18. Ben-Porath I, et al. An embryonic stem cell-like gene expression signature in poorly differentiated aggressive human tumors. Nature genetics. 2008; 40:499–507. [PubMed: 18443585]
19. Possemato R, et al. Functional genomics reveal that the serine synthesis pathway is essential in breast cancer. Nature. 2011; 476:346–350. [PubMed: 21760589]
20. Noda K, et al. Elevated FX expression and increased production of GDP-L-fucose, a common donor substrate for fucosylation in human hepatocellular carcinoma and hepatoma cell lines. Cancer research. 2003; 63:6282–6289. [PubMed: 14559815]
21. Liu W, et al. Reprogramming of proline and glutamine metabolism contributes to the proliferative and metabolic responses regulated by oncogenic transcription factor c-MYC. Proceedings of the National Academy of Sciences of the United States of America. 2012; 109:8983–8. [PubMed: 22615405]
22. De Ingeniis J, et al. Functional specialization in proline biosynthesis of melanoma. PloS one. 2012; 7:e45190. [PubMed: 23024808]
23. Hagedorn CH, Phang JM. Transfer of Reducing Equivalents into Mitochondria by the Interconversions of Proline and Delta1-pyrroline-5-carboxylate. Archieves of Biochemistry and Biophysics. 1983; 225:95–101.
24. Krishnan N, Dickman MB, Becker DF. Proline modulates the intracellular redox environment and protects mammalian cells against oxidative stress. Free radical biology & medicine. 2008; 44:671–81. [PubMed: 18036351]
25. Reversade B, et al. Mutations in PYCR1 cause cutis laxa with progeroid features. Nature genetics. 2009; 41:1016–21. [PubMed: 19648921]
26. Jain M, et al. Metabolite Profiling Identifies a Key Role for Glycine in Rapid Cancer Cell Proliferation. Science. 2012; 336:1040–1044. [PubMed: 22628656]
27. Tibbetts AS, Appling DR. Compartmentalization of Mammalian folate-mediated one-carbon metabolism. Annual review of nutrition. 2010; 30:57–81.
28. Mejia NR, MacKenzie RE. NAD-dependent methylenetetrahydrofolate dehydrogenase is expressed by immortal cells. The Journal of biological chemistry. 1985; 260:14616–20. [PubMed: 3877056]
29. Di Pietro E, Sirois J, Tremblay M, MacKenzie R. Mitochondrial NAD-dependent methylenetetrahydrofolate dehydrogenase-methenyltetrahydrofolate cyclohydrolase is essential for embryonic development. Molecular and cellular biology. 2002; 22:4158. [PubMed: 12024029]
30. Smith GK, et al. Activity of an NAD-dependent 5,10-methylenetetrahydrofolate dehydrogenase in normal tissue, neoplastic cells, and oncogene-transformed cells. Archives of biochemistry and biophysics. 1990; 283:367–71. [PubMed: 2275549]
31. Patel H, Pietro EDi, MacKenzie RE. Mammalian fibroblasts lacking mitochondrial NAD+-dependent methylenetetrahydrofolate dehydrogenase-cyclohydrolase are glycine auxotrophs. The Journal of biological chemistry. 2003; 278:19436–41. [PubMed: 12646567]
32. Lehtinen L, Ketola K, Mäkelä R, Mpindi J. High-throughput RNAi screening for novel modulators of vimentin expression identifies MTHFD2 as a regulator of breast cancer cell migration and invasion. Oncotarget. 2013; 4:48–63. [PubMed: 23295955]
33. Weir DG, Scott JM. The methyl folate trap. The Lancet. 1981; 318:337–340.
34. Linster CL, Van Schaftingen E, Hanson AD. Metabolite damage and its repair or preemption. Nature Chemical Biology. 2013; 9:72–80.
35. Benjamini Y, Hochberg Y. Controlling the false discovery rate: a practical and powerful approach to multiple testing. Journal of the Royal Statistical Society. Series B (Methodological). 1995; 57:289–300.
36. Subramanianan A, et al. Gene set enrichment analysis: a knowledge-based approach for interpreting genome-wide expression profiles. Proceedings of the National Academy of Sciences of the United States of America. 2005; 102:15545–15550. [PubMed: 16199517]
37. Su AI, et al. A gene atlas of the mouse and human protein-encoding transcriptomes. Proceedings of the National Academy of Sciences of the United States of America. 2004; 101:6062–7. [PubMed: 15075390]

38. Kampf C, Olsson I, Ryberg U, Sjöstedt E, Pontén F. Production of Tissue Microarrays, Immunohistochemistry Staining and Digitalization Within the Human Protein Atlas. Journal of Visualized Experiments. 2012; 63:e3620.

39. Chin K, et al. Genomic and transcriptional aberrations linked to breast cancer pathophysiologies. Cancer cell. 2006; 10:529–41. [PubMed: 17157792]

40. Van de Vijver MJ, et al. A gene-expression signature as a predictor of survival in breast cancer. The New England journal of medicine. 2002; 347:1999–2009. [PubMed: 12490681]

41. Desmedt C, et al. Strong time dependence of the 76-gene prognostic signature for node-negative breast cancer patients in the TRANSBIG multicenter independent validation series. Clinical cancer research. 2007; 13:3207–14. [PubMed: 17545524]

42. Pawitan Y, et al. Gene expression profiling spares early breast cancer patients from adjuvant therapy: derived and validated in two population-based cohorts. Breast cancer research. 2005; 7:R953–64. [PubMed: 16280042]

43. Miller LD, et al. An expression signature for p53 status in human breast cancer predicts mutation status, transcriptional effects, and patient survival. Proceedings of the National Academy of Sciences of the United States of America. 2005; 102:13550–5. [PubMed: 16141321]

44. Kao KJ, Chang KM, Hsu HC, Huang AT. Correlation of microarray-based breast cancer molecular subtypes and clinical outcomes: implications for treatment optimization. BMC cancer. 2011; 11:143. [PubMed: 21501481]

45. Cox DRDR. Regression Models and Life-Tables. Journal of the Royal Statistical Society. Series B (Methodological). 1972; 34:187–220.

46. DerSimonian R, Laird N. Meta-analysis in clinical trials. Controlled clinical trials. 1986; 7:177–88. [PubMed: 3802833]

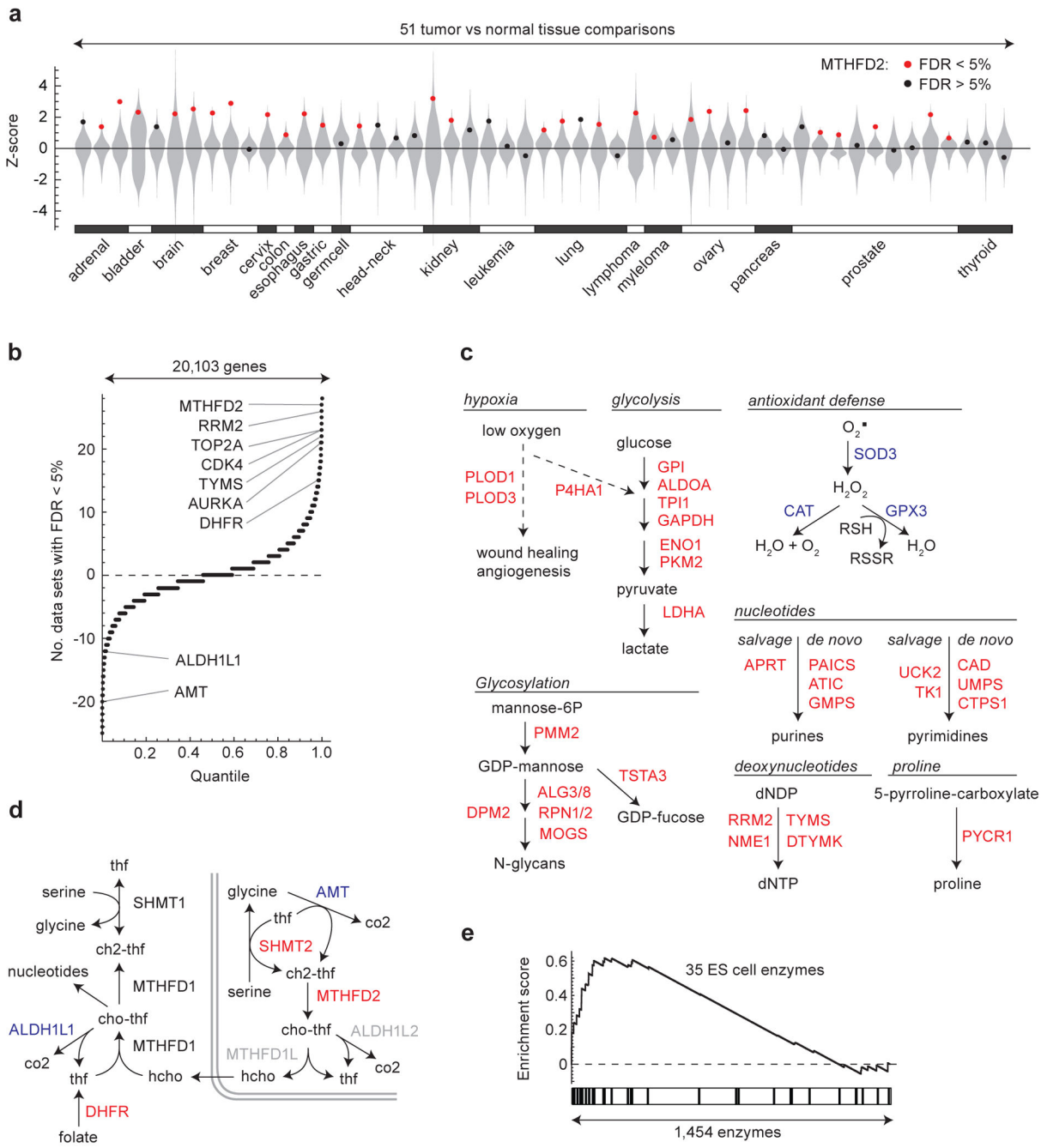

Figure 1. Transcriptional regulation of metabolic pathways in human tumors

(a) Differential expression (Z-score) distributions for 51 tumor-vs-normal data sets representing 19 tumor types are shown as violin plots (gray). Dots indicate Z-score for *MTHFD2* in each study; red color denotes significance at < 5% false discovery rate (FDR). **(b)** Distribution of meta-analysis scores for all 20,103 genes interrogated across the 51 data sets. Gene symbols indicated, see text for further description. **(c)** Metabolic pathways detected as strongly over-expressed (among top 50 metabolic enzymes; red gene symbols) or under-expressed (among bottom 50 metabolic enzymes; blue gene symbols) in tumors.

(d) Schematic of one-carbon metabolism with over-expressed (red) and under-expressed (blue) genes indicated. Gray symbols, not measured. **(e)** Gene set enrichment analysis for the set of 35 embryonic metabolic enzymes compared against mRNAs for all enzymes.

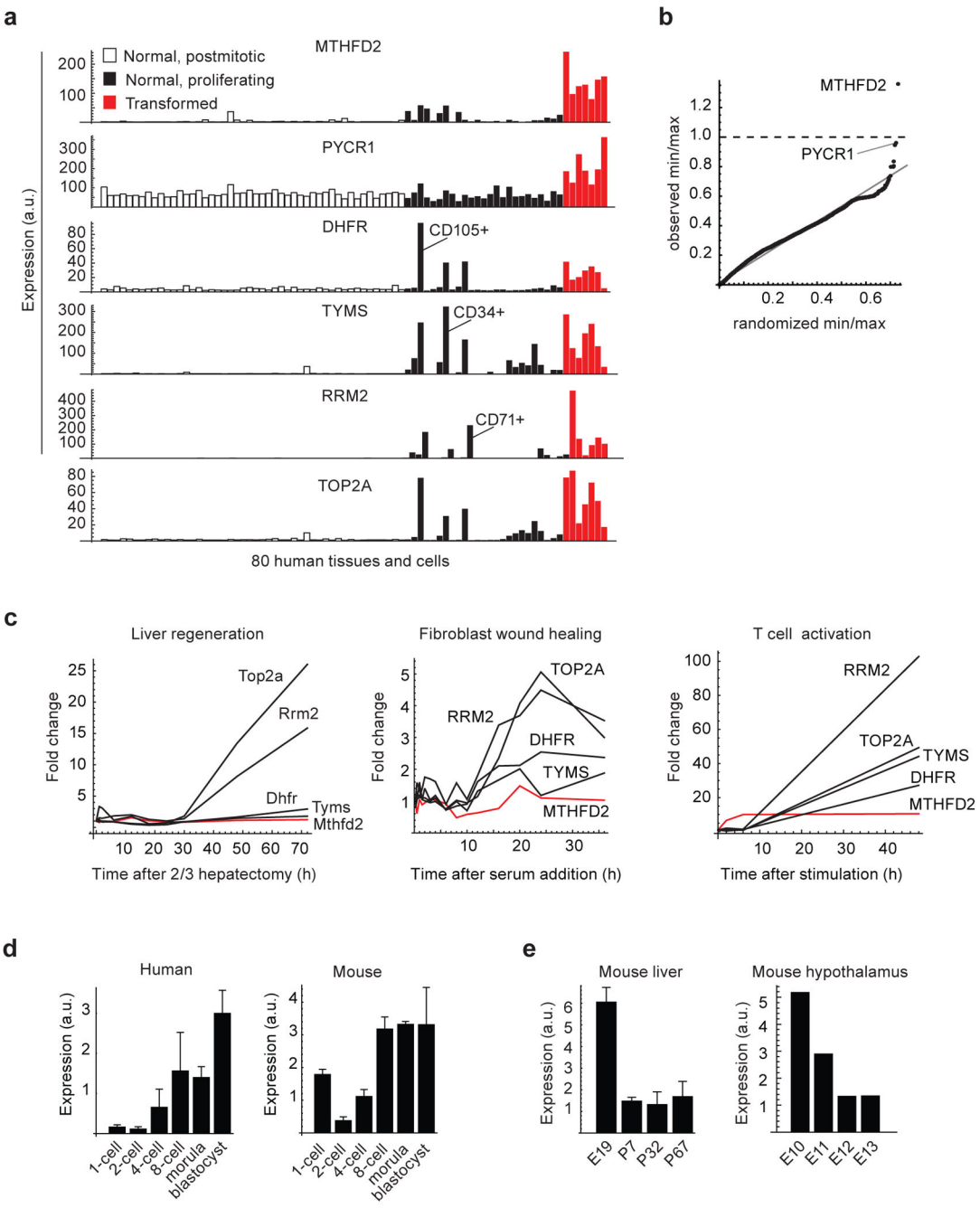

Figure 2. MTHFD2 expression in transformed compared to normal proliferating cells

(a) mRNA expression levels in normal postmitotic (open bars), normal proliferating (black bars) and transformed cells or tissues (red bars) for *MTHFD2* and four established cancer drug targets. Normal hematopoietic cell fractions with strong expression are indicated. **(b)** Quantile-quantile plot for the ratio of minimal expression among transformed cells to maximum expression among normal (proliferating and postmitotic) cells, defined as in (a), for each of the 12,529 human mRNAs measured. Randomized quantiles (X-axis) were obtained by permuting samples. *MTHFD2* mRNA is indicated. **(c)** mRNA expression of

human *MTHFD2* or mouse Mthfd2 and four established cancer drug targets during mouse liver regeneration following partial hepatectomy (left); human fibroblasts proliferating in response to serum stimulation (center); and human CD4+ T lymphocytes activated by CD3 and CD28 antibodies (right). Red line indicates *Mthfd2*/*MTHFD2*. **(d)** mRNA expression of human *MTHFD2* (left) and mouse *Mthfd2* (right) during early embryonic development. Error bars denote standard deviation (n = 3). **(e)** mRNA expression of mouse *Mthfd2* during embryonic development of liver (left) and hypothalamus (right). Error bars denote standard deviation (n = 2).

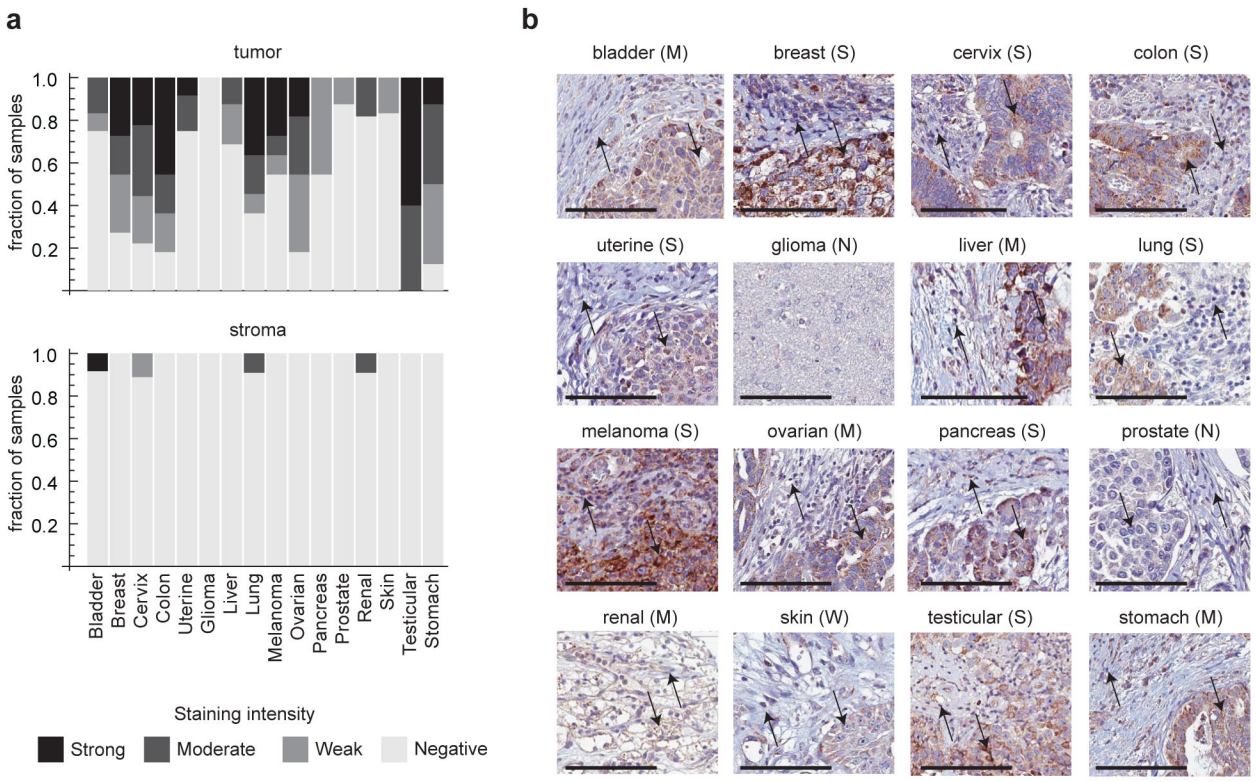

Figure 3. MTHFD2 protein expression in human tumors

(a) Top, fraction of samples with none, weak, moderate or strong immunohistochemistry staining for MTHFD2 in transformed cells, across 16 solid tumor types. Bottom, same analysis as above for stromal cells. For each tumor type, tumors from 9–12 individuals were examined. **(b)** Representative images from each of the 16 tumor types summarized in (a), exemplifying negative (N), weak (W), moderate (M) or strong (S) staining intensities. Up arrow, stromal cells; down arrow, cancer cells. Scale bars represent 100um.

Table 1

Top 50 metabolic enzymes frequently over-expressed in human tumors

Score denotes number of data sets (of 51 total) where each gene was significantly over-expressed at a false discovery rate (FDR) of 5%, as in Fig. 1. Rightmost columns indicate membership in pathways, as in Fig 1.

Score	Symbol	Description	Drug target	One-carbon	Nucleotides	Glycolysis	Hypoxia	Glycosylation
27	MTHFD2	methylene-THF dehydrogenase/cyclohydrolase (mitochondrial)		X				
26	RRM2	ribonucleotide reductase M2	X		X			
25	NME1	protein expressed in non-metastatic cells 1			X			
23	GMPS	guanine monphosphate synthetase			X			
23	SHMT2	serine hydroxymethyltransferase 2 (mitochondrial)		X				
22	GGCT	gamma-glutamylcyclotransferase						
22	UCK2	uridine-cytidine kinase 2			X			
22	TYMS	thymidylate synthetase	X		X			
22	TK1	thymidine kinase 1, soluble			X			
21	PLOD3	procollagen-lysine, 2-oxoglutarate 5-dioxygenase 3					X	
21	ENO1	enolase 1 (alpha)				X		
20	PYCR1	pyrroline-5-carboxylate reductase 1						
20	DNMT1	DNA (cytosine-5-)-methyltransferase 1						
19	FLAD1	flavin adenine dinucleotide synthetase homolog (S. cerevisiae)						
19	ALG3	asparagine-linked glycosylation 3 homolog (S. cerevisiae)						X
19	TSTA3	tissue specific transplantation antigen P35B						X
19	TPI1	triosephosphate isomerase 1				X		
19	RPN2	ribophorin II						X
19	GPI	glucose-6-phosphate isomerase				X		
18	PAICS	AIR carboxylase / SAICAR synthetase			X			
18	DTYMK	deoxythymidylate kinase (thymidylate kinase)			X			
18	ATIC	AICAR formyltransferase/IMP cyclohydrolase			X			
17	MOGS	mannosyl-oligosaccharide glucosidase						X
17	PLOD1	procollagen-lysine, 2-oxoglutarate 5-dioxygenase 1					X	
17	PAFAH1B3	platelet-activating factor acetylhydrolase 1b, catalytic subunit 3						

Nat Commun. Author manuscript; available in PMC 2014 July 22.

Score	Symbol	Description	Drug target	One-carbon	Nucleotides	Glycolysis	Hypoxia	Glycosylation
17	P4HA1	prolyl 4-hydroxylase, alpha polypeptide I					X	
16	RPN1	ribophorin I						X
16	PKM2	pyruvate kinase, muscle				X		
16	LDHA	lactate dehydrogenase A				X		
16	HMBS	hydroxymethylbilane synthase						
16	ALDOA	aldolase A, fructose-bisphosphate				X		
15	SRM	spermidine synthase						
15	GAPDH	glyceraldehyde-3-phosphate dehydrogenase				X		
15	DHFR	dihydrofolate reductase	X	X				
15	CTPS1	CTP synthase 1			X			
15	CAD	carbamoyl-P synthetase 2/aspartate transcarbamylase/dihydroorotase			X			
15	ACLY	ATP citrate lyase						
14	ALG8	asparagine-linked glycosylation 8 (S. cerevisiae)						X
14	CHPF2	chondroitin polymerizing factor 2						
14	UMPS	uridine monophosphate synthetase			X			
14	SRD5A1	steroid-5-alpha-reductase, alpha polypeptide 1						
14	SLC7A1	solute carrier family 7 (y+ system), member 1						
14	PMM2	phosphomannomutase 2						X
14	INPPL1	inositol polyphosphate phosphatase-like 1						
14	APRT	adenine phosphoribosyltransferase			X			
13	CHPF	chondroitin polymerizing factor						
13	B3GAT3	beta-1,3-glucuronyltransferase 3 (glucuronosyltransferase I)						
13	EHMT2	euchromatic histone-lysine N-methyltransferase 2						
13	SLC25A13	solute carrier family 25 (aspartate/glutamate carrier), member 13						
13	DPM2	dolichyl-phosphate mannosyltransferase polypeptide 2, regulatory						X

Table 2

Top 50 metabolic enzymes frequently under-expressed in human tumors

Negative scores denotes number of data sets (of 51 total) where each gene was significantly under-expressed at a false discovery rate (FDR) of 5%, as in Fig. 1.

Score	Symbol	Description
−24	ASPA	aspartoacylase
−23	AOX1	aldehyde oxidase 1
−22	GPX3	glutathione peroxidase 3 (plasma)
−21	ADH1B	alcohol dehydrogenase 1B (class I), beta polypeptide
−20	PTGDS	prostaglandin D2 synthase 21kDa (brain)
−20	MAOB	monoamine oxidase B
−20	AMT	aminomethyltransferase
−19	COX7A1	cytochrome c oxidase subunit VIIa polypeptide 1 (muscle)
−17	UST	uronyl-2-sulfotransferase
−17	SOD3	superoxide dismutase 3, extracellular
−17	PTGIS	prostaglandin I2 (prostacyclin) synthase
−17	ADH1C	alcohol dehydrogenase 1C (class I), gamma polypeptide
−16	PIP5K1B	phosphatidylinositol-4-phosphate 5-kinase, type I, beta
−16	PDE2A	phosphodiesterase 2A, cGMP-stimulated
−16	CYP3A5	cytochrome P450, family 3, subfamily A, polypeptide 5
−16	ALDH2	aldehyde dehydrogenase 2 family (mitochondrial)
−16	ALDH1A1	aldehyde dehydrogenase 1 family, member A1
−15	ECHDC2	enoyl CoA hydratase domain containing 2
−15	DUOX1	dual oxidase 1
−15	ST6GALNAC2	ST6-N-acetylgalactosaminide alpha-2,6-sialyltransferase 2
−15	PPAP2B	phosphatidic acid phosphatase type 2B
−15	PLCL1	phospholipase C-like 1
−15	IDI1	isopentenyl-diphosphate delta isomerase 1
−15	ALDH9A1	aldehyde dehydrogenase 9 family, member A1
−15	ACACB	acetyl-CoA carboxylase beta
−14	MAN1C1	mannosidase, alpha, class 1C, member 1
−14	CHST3	carbohydrate (chondroitin 6) sulfotransferase 3
−14	MAOA	monoamine oxidase A
−14	CYP11A1	cytochrome P450, family 11, subfamily A, polypeptide 1
−14	ATP1A2	ATPase, Na+/K+ transporting, alpha 2 polypeptide
−14	ALDH3A2	aldehyde dehydrogenase 3 family, member A2
−14	ADH1A	alcohol dehydrogenase 1A (class I), alpha polypeptide
−13	NMRK1	nicotinamide riboside kinase 1
−13	INPP5A	inositol polyphosphate-5-phosphatase, 40kDa
−13	HSD11B1	hydroxysteroid (11-beta) dehydrogenase 1

Score	Symbol	Description
−13	CYP27A1	cytochrome P450, family 27, subfamily A, polypeptide 1
−13	CHKB	choline kinase beta
−13	CAT	catalase
−12	ACOX2	acyl-CoA oxidase 2, branched chain
−12	SRD5A2	steroid-5-alpha-reductase, alpha polypeptide 2
−12	SLC6A4	solute carrier family 6 (neurotransmitter transporter, serotonin), member 4
−12	PIK3R1	phosphoinositide-3-kinase, regulatory subunit 1 (alpha)
−12	HMGCS2	3-hydroxy-3-methylglutaryl-CoA synthase 2 (mitochondrial)
−12	GSTM1	glutathione S-transferase mu 1
−12	GATM	glycine amidinotransferase (L-arginine:glycine amidinotransferase)
−12	ETFDH	electron-transferring-flavoprotein dehydrogenase
−12	CDO1	cysteine dioxygenase, type I
−12	ATP6V1E1	ATPase, H+ transporting, lysosomal 31kDa, V1 subunit E1
−12	ATP1B2	ATPase, Na+/K+ transporting, beta 2 polypeptide
−12	SLC25A4	solute carrier family 25 (mitochondrial carrier; ANT), member 4